# The Lorca Earthquake observed by GPS: a Test Case for GPS Seismology

LEONOR MENDOZA[1,2], ALEXANDER KEHM[2], AXEL KOPPERT[2], JOSÉ MARTÍN DÁVILA[1], JORGE GÁRATE[1] & MATTHIAS BECKER[2]

[1] San Fernando Naval Observatory, Cádiz, Spain
[2] Technische Universität Darmstadt, Germany
leonor@roa.es

Recibido: 30/04/2012
Aceptado: 25/09/2012

**Abstract**
1 Hz GPS data recorded by the GNSS network of the Consejería de Agricultura y Agua of the Murcia Region during the Mw 5.1 Lorca earthquake on May 11th 2011 is used as a test case. A Precise Point Positioning (PPP) approach is applied to analyse the earthquake-induced motion of the station LORC, located close to the epicenter. The results are validated using a conventional Double Differences (DD) processing. After applying sidereal and regional filters, the detected transient motion is about 20 millimeters in each component and clearly above noise level. The results from the two different processings are compared in view of the accuracy and applicability.
The PPP approach described here can potentially be used for real-time analysis e.g. based on NTRIP streaming data. It may be used to set up an early warning system, as well as to gain real-time knowledge of ongoing earthquakes, extending the already-existing seismic information obtained from classical measurements.
**Keywords**: Lorca, earthquake, GPS, real-time, PPP, DD, sidereal filter, regional filter.

## Un caso de estudio para la sismología GPS: el terremoto de Lorca

**Resumen**
Se utilizan como caso de estudio los datos de la red GNSS de la Consejería de Agricultura y Agua de la Región de Murcia recogidos a 1 Hz durante el reciente terremoto de Lorca (11 de mayo de 2011, Mw 5.1). Mediante el método de Posicionamiento Puntual Preciso (PPP) se analiza el movimiento inducido en la estación LORC, situada cerca del epicentro. Los resultados se validan usando un procesamiento convencional de Dobles Diferencias (DD). El desplazamiento detectado tras aplicar filtros sidéreo y regional es de aproximadamente 20 milímetros en cada componente, claramente por encima del nivel de ruido. Los resultados obtenidos mediante ambos métodos se comparan en función de su precisión y aplicabilidad.
La metodología PPP aquí descrita puede enfocarse hacia el análisis en tiempo real mediante, por ejemplo, un flujo de datos con protocolo NTRIP. También puede usarse para instalar un sistema de alerta temprana, así como para proporcionar información sobre terremotos en curso y ampliar la información ya existente, obtenida por métodos clásicos.
**Palabras clave**: Lorca, terremoto, GPS, tiempo real, PPP, DD, filtro sidéreo, filtro regional.




ISSN: 0214-4557
http://dx.doi.org/10.5209/rev_FITE.2012.v24.40135

**Referencia normalizada**
Mendoza, L., Kehm, A., Koppert, A., Martín Dávila, J., Gárate, J. and Becker, M. (2012). The Lorca Earthquake observed by GPS: a Test Case for GPS Seismology. *Física de la Tierra*, Vol. 24, 129-150.

## Introduction

The $M_w$ 5.1 Lorca earthquake that took place on 11th May 2011 was successfully recorded by one of the GPS receivers belonging to the local GPS network from the Consejería de Agricultura y Agua of the Murcia Region (Meristemum, http://gps.medioambiente.carm.es). This receiver was optimally located - only 5 km away from the epicenter - to record the ground motion produced by the seismic waves related to the event. The hypocenter was located between 1 and 2 km in depth, and less than 2 km away from the city of Lorca. The largest foreshock ($M_w$ 4.5) happened two hours before the main event and was located 5 km east-northeast from the city. Moreover, there were seven aftershocks with magnitudes between $M_w$ 2.6 and 3.9: four on the evening in the same day; two on 14th May; and one on 15th May (European Mediterranean Seismological Center, www.emsc-csem.org/).

Although a $M_w$ 5.1 earthquake is not considered a dangerous threat due to its medium size, it led to some casualties. The large damage was mainly caused by the shallowness of the hypocentre and its closeness to the city. Nearly 250 people were injured. The earthquake caused structural damage to many buildings in the city of Lorca, including the collapse of an old monastery. The $M_w$ 4.5 foreshock could have weakened the buildings leading to major damage in consequence of the main shock (Cabañas-Rodríguez *et al.*, 2011).

The present paper briefly introduces the tectonic setting of the region and the location of the GPS receivers from the Meristemum network. The results from two different processing strategies are compared. We use two independent software suites: RTKLIB with a Precise Point Positioning (PPP) approach and the Bernese software for Double Differencing (DD). For a better separation of the earthquake-induced station motion from the noise, a modified sidereal filter and a regional filter are implemented. Finally, the first steps towards a PPP real-time procedure are explained in detail.

This study is of utmost interest for three reasons. First, the Lorca earthquake is one of the few medium-size events successfully recorded by GPS. Second, we show that this is feasible using a PPP approach instead of a conventional DD processing. And third, an insight into a real-time application of the PPP methodology is provided.

## 1. Tectonic Setting of the Zone and Location of the GPS Receivers

The province of Murcia, population 1,470,069 on January 2011 (Instituto Nacional de Estadística, www.ine.es), is located in the South-East of Spain, directly in the Betic Cordillera and close to the area where the Eurasian and African (Nubian) plates converge (Dewey *et al.*, 1973). The Betic Cordillera was generated by a series of collisions and separations between the aforementioned tectonic plates, with an overall deformation between 0 and 4 mm/yr (Khazaradze *et al.*, 2007). Such a complex history leads to a dense network of secondary faults instead of a major contact fault. Since the overall stress diverges to those small faults, earthquakes of small magnitude are predominant (Buforn *et al.*, 1995). Nevertheless, the existence of some medium-to-large faults indicates that the occurrence of major earthquakes ($M_w$ 6.0) cannot be dismissed (García-Mayordomo *et al.*, 2007).

The city of Lorca is located next to a main fault zone called the Lorca-Totana fault, commonly known as the Alhama de Murcia fault. It belongs to a NE-SW trending network of prominent faults characterized by marked seismicity. This network extends up to the Alboran Sea in a belt of equally high seismic activity (Vissers and Meijninger, 2011).

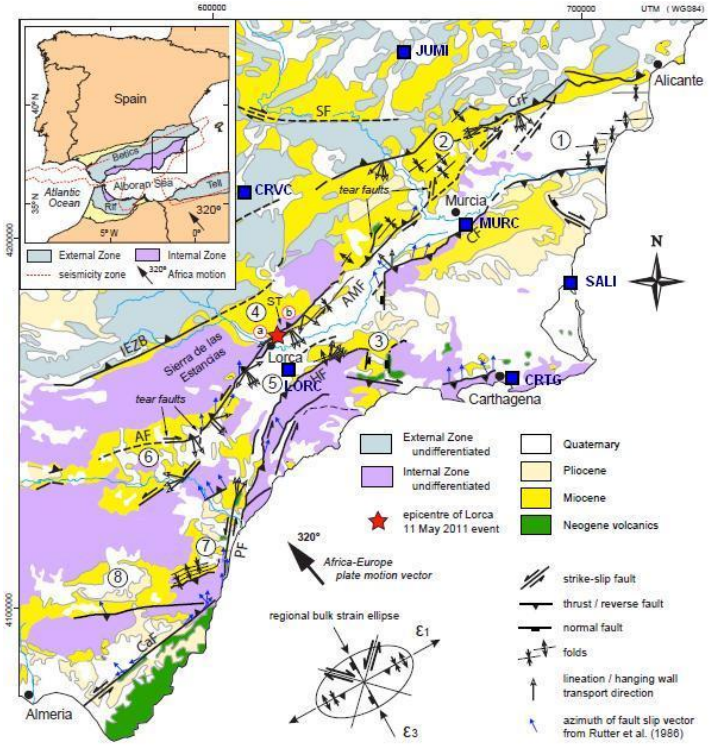


Fig. 1. Tectonic Settings of the Province of Murcia. Map modified from Vissers and Meijninger (2011).

Fig. 1 shows the complex tectonic distribution of SE Spain. Number (4) indicates the Lorca basin. The point marked as "Lorca" corresponds to the location of the city. The star shows the epicenter of the earthquake. The squares, each with a 4 character label, point to the location of the different Meristemum GPS stations. The epicentral distances to the stations are shown in Table 1. The African-European plate motion vector is taken from DeMets *et al.* (1994). Further explanations about the figure can be found in the paper from Vissers and Meijninger (2011). The full-color map can be found in the online version of this publication (http://dialnet.unirioja.es/servlet/revista?codigo=1519).

Tab. 1. Considered stations of the GPS network Meristemum

| **Station** | | **Epicentral distance (km)** |
|---|---|---|
| CRTG | Cartagena | 62 |
| CRVC | Caravaca de la Cruz | 49 |
| JUMI | Jumilla | 91 |
| LORC | Lorca | 5 |
| MURC | Murcia | 58 |
| SALI | San Pedro del Pinatar | 80 |

## 2. Processing Strategies

The potential of GPS data has increased with the development of the receivers capacity of recording, storing and transferring data up to 50 Hz. One Hertz sampling rate has been proven a very valuable resource for precise analysis of short-duration events such as large-magnitude earthquakes like 2002 Denali (Kouba, 2003 and Bock *et al.*, 2004), 2004 Sumatra-Andaman (Ohta *et al.*, 2006), 2011 Japan (Grapenthin and Freymueller, 2011 and Pollitz *et al.*, 2011) and earthquake-induced tsunamis like 2004 Kii (Kato *et al.*, 2005), 2011 Japan (Yamazaki *et al.*, 2011).

The most commonly used approaches to precise GPS data analysis are Precise Point Positioning (PPP) and Relative Positioning or Double Differences (DD). The station position with respect to a global terrestrial reference frame can be estimated by different means in both strategies. The Bernese GPS Software (Beutler *et al.*, 2008) is used to process baselines, two of them presented in this paper: MURC-LORC and CRVC-MURC. The first baseline is perpendicular to the fault, and the latter parallel to it. Only after confirming that there is no visible displacement in the station MURC for baselines CRVC-MURC and JUMI-MURC, and double-checked with the solutions obtained with PPP, it was used as fixed station for baseline MURC-LORC. The RTKLIB Software (Takasu, 2011) is used to obtain PPP solutions for the stations in the network (CRTG, CRVC, JUMI, LORC, MURC and SALI, see Fig. 1). More stations are processed by PPP in order to get a proper regional filter. The results are analyzed and compared in the following subsections.

PPP provides absolute positioning, i.e. it enables the estimation of precise site coordinates and receiver clock corrections independently for each station analyzed. Since the process is based on undifferenced code and phase observations, the quality of the clocks and orbit information used in the processing is essential.

On the other hand, DD is based on a relative positioning strategy which allows the estimation of site coordinates simultaneously for a whole network, using double-differenced observations (baselines) and resolving the integer-cycle phase ambiguities to their correct integer values (Beutler *et al.*, 2008). The use of double differences leads to a cancellation of both GPS receiver and satellite clock errors. Therefore, high accuracy in clock data is not necessary. This procedure can achieve high precision for the relative geometry between the sites processed in a network solution. However, DD is computationally more intense than PPP.

### 2.1. PPP Processing in RTKLIB

For PPP processing we used the program RTKPOST, which is part of the open-source program package RTKLIB (Takasu, 2011). We processed the two-frequency observation data using the ionosphere-free linear combination in RTKPOST kinematic PPP mode. The (Kalman-) filtering was carried out forwards and backwards (so-called combined) to eliminate convergence effects. We used the IGS Final orbit (15 minutes sampling) and clock products (30 s sampling). The use of the IGS products implies that the obtained coordinates are in ITRF. A tropospheric zenith path delay and gradients were estimated by the program. Antenna corrections were applied using the latest IGS ANTEX file (ANTEX08.atx). Additionally, the differential code biases were taken into account using the data provided by CODE (Center for Orbit Determination in Europe). The processing was done on a daily basis, starting at 0:00 GPS time (GPST). As the earthquake occurred at around 16:47 GPST, we assume that the filter has fully converged at that time, thus PPP should have reached its full precision. RTKLIB version 2.4.1 used for this study is not capable to resolve ambiguities in PPP mode.

### 2.2. DD Processing with the Bernese Software

For DD processing we used the program Bernese GPS Software version 5.0 (Beutler *et al.*, 2008). In a first step, we applied a standard procedure to obtain mean coordinates for two stations forming a baseline. Troposphere parameters are also estimated. For the considered baselines, the best-fit cycle-slip resolution strategy is the so-called Narrowlane-Widelane. In this strategy, first a real-value ambiguity estimation is achieved. And, in a second step, the ambiguities are resolved as integers and the mean coordinate for the considered timespan (24 hours, starting at 00:00 GPST) is obtained. We used IGS Final orbit (15 minutes sampling) and earth rotation parameters for GPS week 1635, as well as ionospheric information downloaded from CODE. After solving the ambiguities, we run a batch kinematic processing in Bernese for each baseline, where the integer ambiguities of the first step are introduced. The coordinates of the reference station in each baseline are

held fixed in order to estimate the coordinates of the kinematic station. As well as for the PPP approach, the computed coordinates are referred to ITRF.

## 3. Sidereal and Regional Filters

High-Rate GPS positioning precision is influenced by GPS measurement noise, the number and location of the satellites, as well as the ability to model errors associated with orbits, satellite and receiver clocks, atmospheric delays, antenna effects and signal multipath (Choi *et al.*, 2004). The application of the following filters leads to a separation of the earthquake signal from a great part of the noise inherent to the GPS recording.

### 3.1. Modified Sidereal Filter

The goal of the Modified Sidereal Filter (MSF) is the elimination of all effects influencing the position solutions, which occur periodically with the satellite constellation (e.g. multipath). This means, effects not being caused by the specific satellite constellation remain in the filtered positions.

The GPS satellite constellation at a specific location repeats at intervals of approximately one sidereal day. MSF is based on the period of the satellite constellation being about 8 s shorter than one sidereal day (Choi *et al.*, 2004). This period, called Aspect Repeat Time (ART) (Agnew and Larson, 2007), represents the time a satellite needs in an earth-fixed reference frame to return to a position of minimal distance to the starting position (i.e. same azimuth and elevation). For the determination of the Aspect Repeat Times of the satellites we used the program ASPREP (Agnew and Larson, 2007).

We calculated the ART of the single satellites for the reference position of the station LORC and the reference time day 131, 16:47 GPST (the time of the earthquake). The period of the satellite constellation was obtained as the arithmetic mean of the ART of all satellites, and had a value of T = 86155 s (rounded to integer number of seconds).

#### 3.1.1. Routine of the Modified Sidereal Filter

The timespan of interest is DOY 131, 15:30 to 17:30 GPST. For the MSF, we considered the epoch-wise residuals $\Delta \boldsymbol{X}_t = (\Delta X_t \;\; \Delta Y_t \;\; \Delta Z_t)^{\mathrm{T}}$ between the kinematic position solutions and their daily mean.

Here, MSF for one station is based on its position time series for the whole GPS week 1635.

First, for every epoch t of the considered timespan of DOY 131, the epochs in intervals of integer multiples of the ART ($t \pm n\,T$) are searched. These are the corresponding epochs at each of the other days within GPS week 1635, as their satellite constellation is the same as at the filtered epoch. Afterwards, the residuals of these corresponding epochs $\Delta \boldsymbol{X}_t$ are arithmetically averaged (stacking) and subtracted from the solution of epoch t.

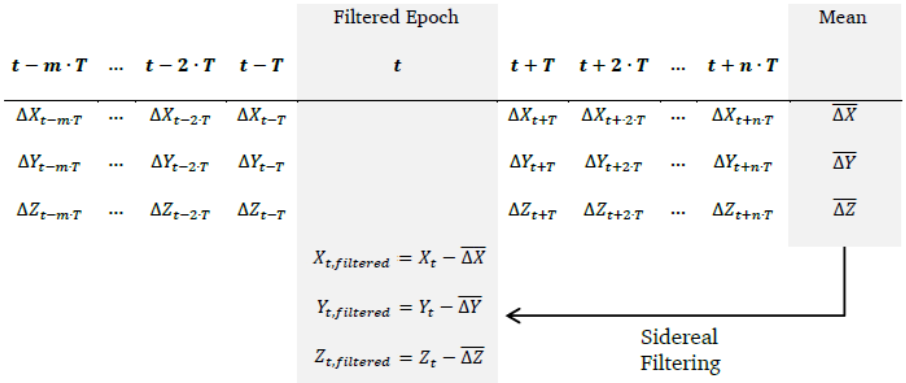


Fig. 2. Scheme of modified sidereal filtering for one station and one epoch.

As the solutions for DOY 134 were of bad quality, we did not use them for the MSF. For real-time applications, this filter can only be performed using data already available.

Note that sidereal filtering relies on an unchanging environment at the site. In case of significant changes (e.g. collapse of buildings) multipath effects will change. In this case, the assumption of periodicity of these effects is no longer valid (with reference to the epochs previous to the event). In our case, no significant variations or permanent displacements at the considered stations were recorded after the earthquake. Thus, for the Lorca earthquake, sidereal filtering can be applied using pre- and post-earthquake data.

### 3.2. Regional Filter

In order to remove the spatially correlated influences, we subjected the sidereally filtered PPP solutions to a Regional Filter (RF). The goal is to remove occasional and deterministic common-mode effects influencing all stations in the area in a similar way, but not being related to the periodically repeating satellite constellation. The region around the filtered station should include all neighbouring stations within a range of a few hundred kilometers to eliminate residual effects from orbit errors, loading and other common biases. When double-differencing (DD), these effects deteriorating the station positions are intrinsically removed and do not need to be filtered again.

The concept of RF follows the paper from Wdowinski *et al.* (1997), where this technique is introduced as spacial filtering. As we are dealing with 1-Hz data for a short period of time (the timespan of interest is again DOY 131, 15:30 to 17:30 GPST), the algorithm is slightly modified.

Initially, for all stations in the reference network, we computed the differences $\Delta X_{S,t}$, $\Delta Y_{S,t}$, $\Delta Z_{S,t}$ of the epoch-wise solution to a reference solution from static PPP processing. Then, we averaged the residuals over all stations involved and subtracted the resulting data from the station epoch solution (see Fig. 3).

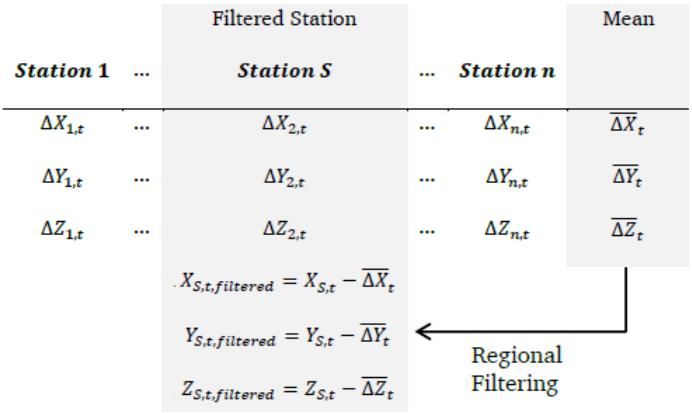


Fig. 3. Scheme of regional filtering for one epoch.

## 4. Case of Study: The Lorca Earthquake

The solutions for PPP and DD after MSF, as well as after MSF and RF, will be compared for the data processed from the Lorca earthquake. The timespan filtered goes from 15:30 to 17:30 GPST, on 11th May, 2011 (DOY 131). The time of the earthquake is 16:47 GPST.

### 4.1. Data

The stations of the Meristemum network deliver GPS observation data in RINEX format with a frequency of 1 Hz. The data is available from the open-access FTP server ftp://meristemum.carm.es/GPS.

For a suitable MSF and RF, data from the surrounding GPS stations as well as for the days around the event are essential. Therefore, we downloaded the RINEX data for GPS week 1635, containing the days 128 to 134 of year 2011, from all the stations available in the Meristemum network.

We also fetched IGS Final products, including precise orbit information in SP3-c format and earth rotation parameters in ERP format as well as 30-second clock data, from ftp://cddis.gsfc.nasa.gov/gps/products/1635.

From CODE, we also downloaded ionospheric information for each day and the data necessary to correct the differential code biases.

### 4.2. Processing of the Data

As explained in section 3, filters are implemented to reduce noise in the position time series, in order to clarify the earthquake-induced displacement of the GPS station. The short-periodic noise can be characterised computing the empirical standard deviation $S_N$ of the positions. Therefore, a reduction in $S_N$ can be interpreted as a reduction of noise level. A reliable detection of the stations displace-

ments by the seismic waves is only possible if the noise level is smaller than the displacement.

### 4.2.1. DD Results Computed by Bernese with MSF

The medium-length baselines considered are CRVC-MURC (66.7 km) and MURC-LORC (62.1 km). For such lenghts, the best strategy for ambiguity resolution is the so-called Widelane-Narrowlane (Beutler *et al.*, 2008). The ratio of ambiguities solved is a 96.4 % for CRVC-MURC and a 89.3 % for MURC-LORC on the day of the earthquake. We use this same strategy to process both baselines for the seven days of the GPS week considered. A distinct reduction of the scatter in the baseline solutions is obtained after applying the MSF.

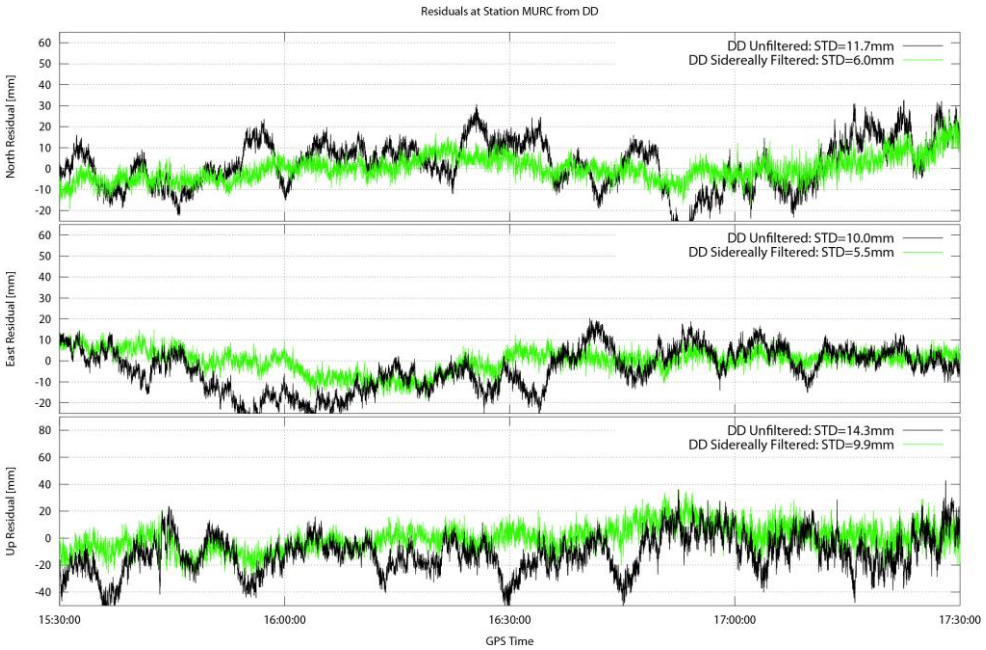


Fig. 4. DD time series, station MURC.

The reduction in empirical standard deviation is 55 % and 48.7 % in N-S, 42.7 % and 45 % in E-W and 39 % and 30.8 % in the vertical components for stations MURC and LORC, respectively, after MSF. This is a reduction between 4 and 6 mm in the position and height components for both stations (see Table 2).

### 4.2.2. PPP Results Computed by RTKLIB with MSF and RF

For the stations of the considered network (CRTG, CRVC, JUMI, LORC, MURC, SALI) kinematic PPP solutions have been computed using RTKLIB for all days of GPS week 1635 on a daily basis. First, MSF was applied to all solutions. For the

subsequent reduction of common-mode errors via RF all stations mentioned above were considered. We present the results for LORC and MURC (Fig. 5).

By applying the combined MSF and RF filters the empirical standard deviation is reduced by 13 mm in N-S, 7 mm in E-W and 35 mm in height (68-77 % reduction in N-S and E-W and 79 % in height) for station MURC. On the other hand, for station LORC the reduction is only 5 % in E-W direction, but of a 51 % in N-S and 15 % in height (see Table 2).

We find that the combined correction (MSF and RF) applied to PPP reduces the standard deviation by 10-12 % more than when using the MSF only (see Table 2). Such results highlight the usefulness of both filters applied at the same time to PPP.

Standard deviations after MSF show the same level for all stations considered. This means that the filter reduced most of the site-dependant effects.

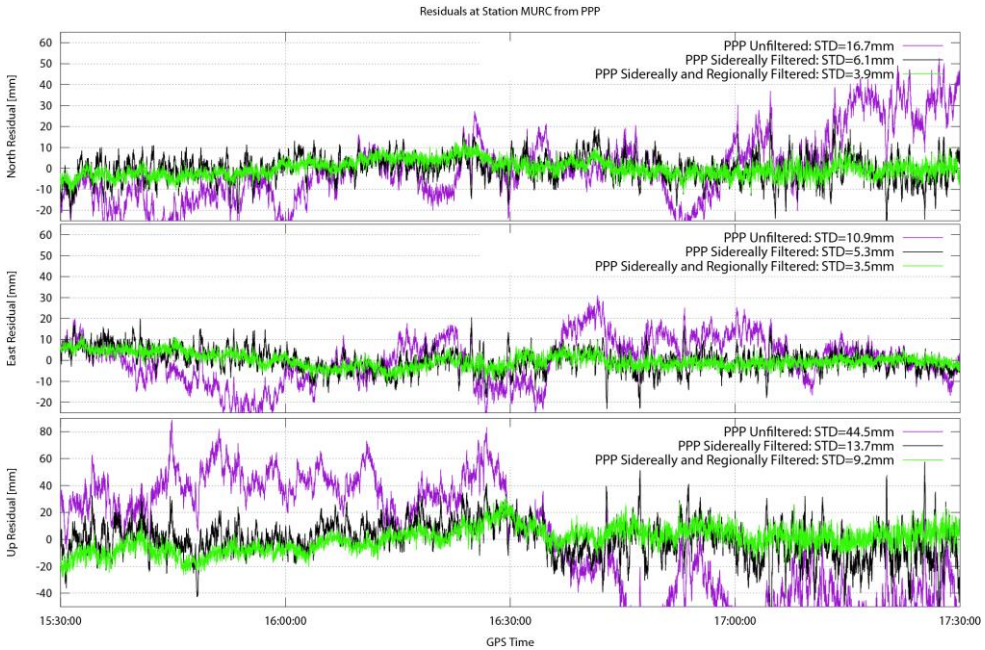


Fig. 5. PPP time series, station MURC.

### 4.3. Comparison Between Strategies and Filters

After the MSF, a minimization of the effects related to the satellite-receiver geometry (multipath) is achieved, eliminating site-dependant effects. RF eliminates spatially correlated effects, this is, noise that repeats in the region, cancelling most of the high-frequency noise and common trends.

In order to compare the different results, Table 2 shows the empirical standard deviations $S_N$ for the two hours around the event (from 15:30:00 to 17:30:00) and

each strategy and filter. In addition, the ratio of reduction in the standard deviation is also presented for each applied filter.

Tab. 2. Empirical Standard Deviations for LORC and MURC stations, DD and PPP, and applied filters. Ratio of improvement between unfiltered and filtered solutions. Time interval considered: from 15:30:00 to 17:30:00 GPST

| | | **DD Raw (mm)** | **DD MSF (mm)** | **%** | **PPP Raw (mm)** | **PPP MSF (mm)** | **%** | **PPP MSF,RF (mm)** | **%** |
|---|---|---|---|---|---|---|---|---|---|
| **LORC** | $S_N$ **N-S** | 12.0 | 5.4 | **55.0** | 7.8 | 6.4 | 17.9 | 3.8 | **51.3** |
| | $S_N$ **E-W** | 7.5 | 4.3 | **42.7** | 5.9 | 6.5 | -10.2 | 5.6 | **5.0** |
| | $S_N$ **Up** | 13.6 | 8.3 | **39.0** | 14.1 | 13.6 | 3.5 | 12.0 | **14.9** |
| **MURC** | $S_N$ **N-S** | 11.7 | 6.0 | **48.7** | 16.7 | 6.1 | 63.5 | 3.9 | **76.6** |
| | $S_N$ **E-W** | 10.0 | 5.5 | **45.0** | 10.9 | 5.1 | 53.2 | 3.5 | **67.9** |
| | $S_N$ **Up** | 14.3 | 9.9 | **30.8** | 44.5 | 13.7 | 69.2 | 9.2 | **79.3** |

Note that empirical standard deviation is calculated applying the formula:

$$S_N = \sqrt{\frac{1}{N-1}\sum_{i=1}^{N}(x_i - \bar{x})^2}$$

where $N$ is the number of samples (in this case, number of seconds in the 2 hours interval), $x_i$ each value and $\bar{x}$ the mean of the values.

Comparing the results after a MSF, it is clear that DD sidereally filtered leads to better standard deviations than PPP filtered in the same way for both stations (but not for Murcia in the E-W component, where a standard deviation of 5.5 mm is found in DD after MSF, bigger than the 5.1 mm obtained after using the same filter for PPP).

On the other hand, when applying both MSF and RF to the PPP solutions, the results improve compared to DD after MSF for MURC station, and also for LORC in the N-S direction. Nevertheless, DD after MSF is still better for LORC station for E-W and vertical components. Therefore, no clear outcome can be stressed.

The scatter reduction for station MURC can be seen in Fig. 6.

### 4.4. The Earthquake

In Fig. 7, the filtered results within two minutes around the time of the earthquake are shown. For both N-S and E-W components we can see that, during the event, the solutions show similar behaviour when processed by PPP and DD.

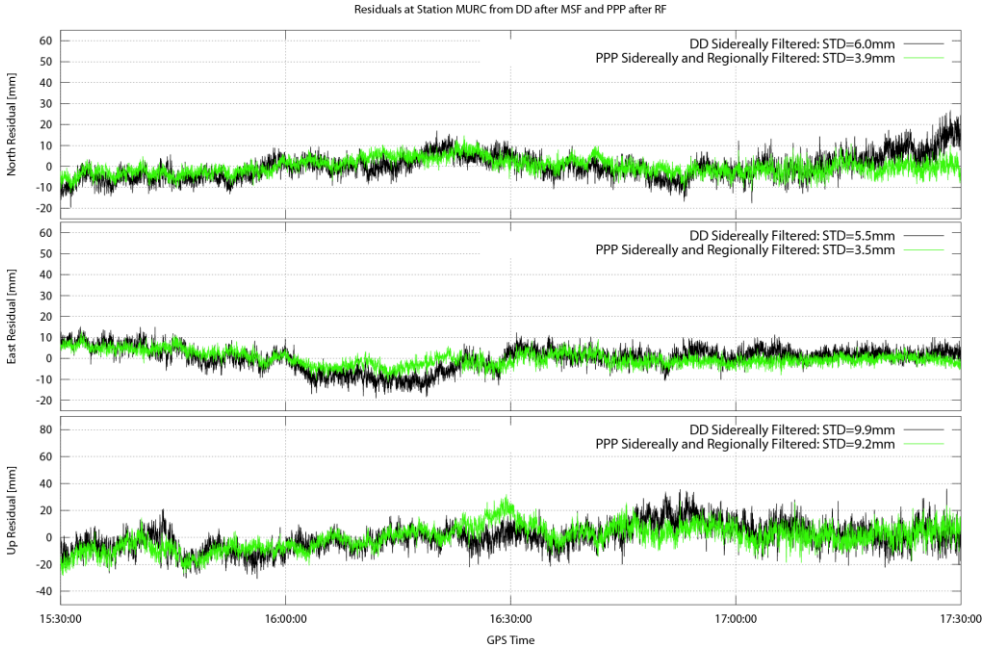


Fig. 6. Comparison DD and PPP for the station MURC.

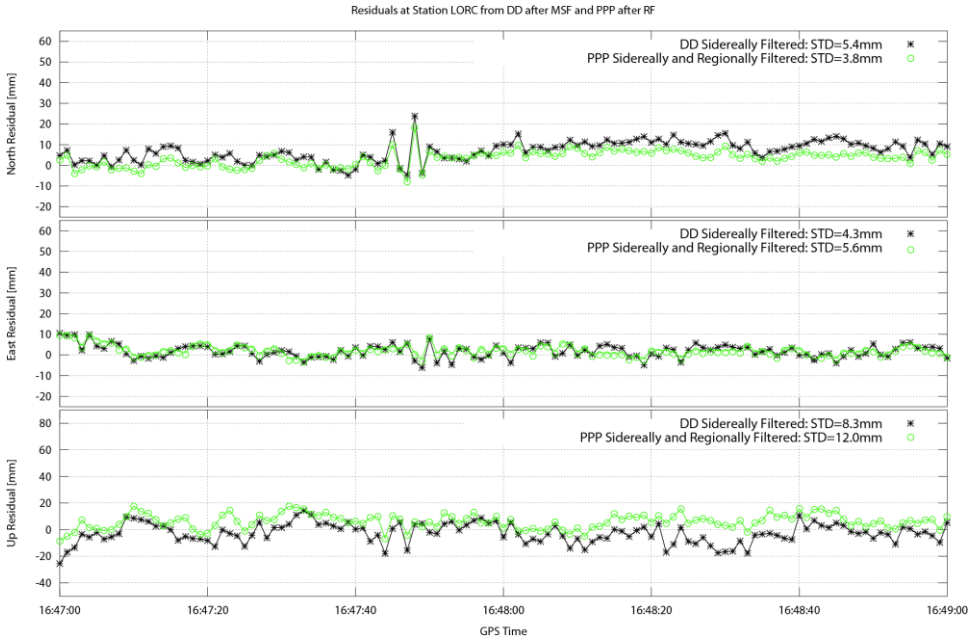


Fig. 7. LORC time series for the time around the earthquake (16:47:40 GPST).

The first solution from both PPP and DD for the station LORC (Fig. 7), shows a peak-to-peak movement with two to three centimeters in N-S direction, and less than two centimeters in E-W direction, as well as in height. The amplitude of the signal (~1.5 cm for N-S, ~0.8 cm in E-W, amplitude defined as the half of the peak-to-peak displacement) remains constant after filtering.

The earthquake happened at 16:47:25 UTC, that is 16:47:40 GPST. GPST is 15 seconds ahead of UTC time. Moreover, the station LORC is placed 5 km away from the epicenter, thus the expected time of arrival of the first seismic wave is a few seconds after the initiation of the event. The first motion that we can clearly relate to the seismic waves occurs at 16:47:42 GPST in LORC, 5 km away from the epicenter. This is 2 s after the time of origin published by US Geological Survey (http://earthquake.usgs.gov/earthquakes/eqinthenews/2011/usc0003c5s/). Thus, the approximated arrival of the same wave group at MURC, placed 58 km away, is at 16:48:02 GPST. For this station, the earthquake signal cannot be separated from the noise. The biggest foreshock at 15:05 UTC is not visible either, neither in sidereal filtered DD nor in sidereal and regional filtered PPP solutions.

### 4.5. Polar Plots

For a further examination of the earthquake-induced movements of the station LORC, the ground track of the computed positions from the PPP processing (cf. 4.2.2) is visualized in Fig. 8. Only horizontal displacements are considered here over a timespan of 15 seconds. This view can help us to study the properties of the seismic waves and it ideally allows the identification of their type. In order to do that, we have to relate the station motion to the direction of propagation of the seismic waves. Assuming a direct radial propagation of the seismic waves (because of the closeness to the epicenter and the minor depth of the hypocenter), the direction of propagation can be approximated by the azimuth between the earthquake epicenter and the station site (193.6°).

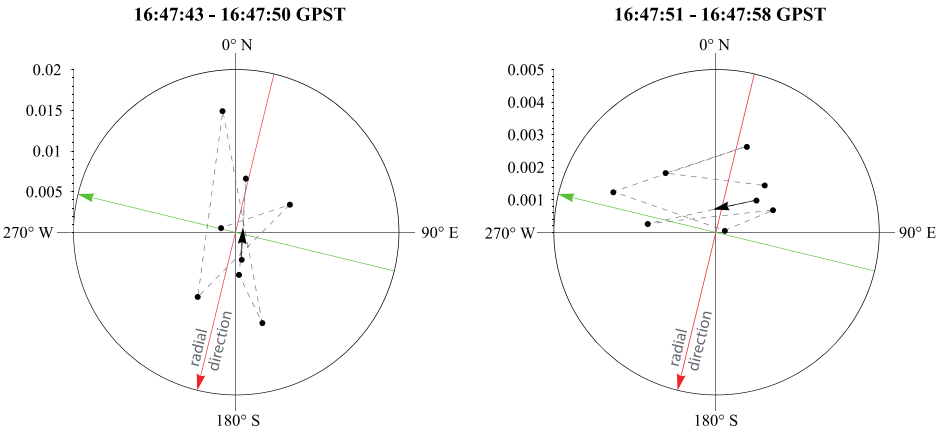


Fig. 8. Polar Plots from station LORC.

Between 16:47:43 and 16:47:50 GPST the station mainly undergoes movements in radial direction with amplitudes up to 2 cm. After 5 seconds also a smaller perpendicular movement becomes visible. During the following 8 seconds (16:47:51 - 16:47:58 GPST) the main direction of movement is perpendicular to the computed direction of wave propagation (perpendicular to the radial direction), but there is also a noticeable radial movement. The displacements during this period are generally smaller than during the period before (note the different scaling of the two figures).

There are obviously systematic displacements of the station LORC which can be related to the assumed direction of propagation of the seismic waves. The displacements before and after this period do not show this systematic nature (cf. Fig. 7). As we observe radial as well as tangential displacements, the waves studied here can be identified as surface waves. This observation is consistent with the minor depth of the hypocenter which lead to big surface waves (Vissers and Meijninger, 2011). The body waves have been too small to be identified in our position time series.

## 5. Towards Real-Time Earthquake Monitoring and Early Warning

The importance of real-time GPS data for earthquake and tsunami early warning is described by several authors (e.g. Blewitt *et al.*, (2006); Falck *et al.* (2010); Allen and Ziv (2011)). As there is a high seismic activity in the Mediterranean countries (Papadopoulos and Fokaefs, 2005) as well as a non-negligible risk of earthquake-induced tsunamis in the Mediterranean Sea (Tinti *et al.* (2005) and Sørensen *et al.* (2012)), we discuss how the results presented in the previous sections could be obtained in real-time to support an early warning system in this region.

From the distribution of the seismic faults capable to produce an ocean-wide tsunami as described by Tinti *et al.* (2005) and Sørensen *et al.* (2012) we can see that the network considered here can only be a small part of the station network needed to form a tsunami early warning system in the western Mediterranean region. For example a risk for the Spanish coast and the Balearic Islands arises mainly from Algeria (Tinti *et al.*, 2005). Hence our work should only be considered as a test case for an efficient real-time processing of GPS data using PPP within such a system, delivering GPS stations position time series for further seismological studies. If this information is available in real-time, it can help to assess the potential hazard of an earthquake or tsunami, and could contribute to an early warning process. In addition, Blewitt *et al.* (2006) and Allen and Ziv (2011) (among others) present how the magnitude estimation can be performed using the permanent displacement of GPS stations.

There are two key requirements to meet: real-time data transmission and real-time data processing, including the infrastructure needed for real time orbit and clock estimation (Blewitt *et al.*, 2009).

### 5.1. Real-Time Data Transmission

Nowadays, the NTRIP standard (Networked Transport of RTCM Data via Internet Protocol) allows the transmission of GNSS data in real-time via the internet. GNSS observations, as well as precise orbit and clock information required for processing, can be broadcast by means of data streams in RTCM format (Schmitz, 2010). For more detailed information about NTRIP see Weber *et al.* (2005).

1-Hz observation data of the permanent stations belonging to the Meristemum network are disseminated as NTRIP streams (http://gps.medioambiente.carm.es /tiemporeal.php) and are made available through the caster gps.medioambiente.carm.es. Thus, the needed real-time high-rate data are already available for earthquake monitoring in the test area and it is to be expected that more stations will switch to NTRIP streams in future.

### 5.2. Real-Time Data Processing

The processing techniques described above (PPP, DD, MSF and RF) are all suited for real-time applications. The program library RTKLIB, which we used for the PPP postprocessing, supports also the real-time processing using NTRIP data streams (RTKNAVI) (Takasu, 2011). Therefore it could be part of the real-time workflow. In postprocessing we used the IGS Final products but as they are only available with a latency of 12-18 days, they cannot be used for real-time applications. Alternatively real-time correction streams can be used. These are provided by different analysis centers contributing to the IGS Real-Time Pilot Project (IGS-RTPP, http://www.rtigs.net). These precise corrections in RTCM format, which have to be applied to the broadcast ephemeris, are made available via NTRIP caster products.igs-ip.net. The quality of these streams is lower than the quality of the IGS Final products and this may decrease the accuracy of the PPP positioning. This effect will be discussed in the following section.

The real-time position determination with RTKLIB in PPP mode can be followed by a sidereal filtering in the coordinate domain using the positions of the previous days without limitations due to the real-time environment. The RF of the sidereal filtered PPP solutions would also be possible. It is important to note that for RF, a sufficient number of stations not affected by the seismic waves is necessary. Only these stations can be used for filtering without deteriorating the seismic signals at the considered site.

As the Lorca earthquake only induced significant displacements at the station LORC, our work was not concerned by this problem. For real-time RF and large earthquakes, it would be essential to implement a strategy to eliminate the stations showing any earthquake-related movement from the filtering process.

For early warning we are interested in the timespan between the earthquake event i.e. its origin time and the warning which is based on reliable information about the event. The real-time processing duration described here is calculated as the sum of the observation stream latency plus the time needed for processing and filtering. Due to its short duration, the latter can be neglected. The latency of the observation streams is less than 3 seconds (Dettmering and Weber, 2004), thus

with a latency of slightly more than 3 s the station positions are already available for further seismological studies. This is much less than for example the time needed for a batch-processing in Bernese of the already existing GPS component of GITEWS (German Indonesian Tsunami Early Warning System) which starts every two minutes (Falck *et al.*, 2010).

Now, we focus on the positioning accuracy that can be obtained in real-time.

### 5.3. Test Case: Lorca Earthquake

We reprocessed the observation data of the LORC station under real-time conditions in PPP mode. The processing is based on data that could have been available at the time of the earthquake. We used the predicted part of the IGS Ultra-Rapid orbits and a combination clock product, which is computed within the framework of the IGS-RTPP. The combination is based on the real-time clock products provided by the participating analysis centers (and which are available for the user as NTRIP streams in real-time). The individual AC solutions are available only from GPS week 1677 on (IGS Real Time Pilot Project Analysis Centre Datasheet ftp://nng.esoc.esa.de/RTPPdata/IGS%20Real%20Time%20Pilot%20Project%20Data%20Sheetsv10.doc) so they could not be used within this test. The PPP result obtained under these real-time conditions is now compared to our PPP reference solution from section 4 above.

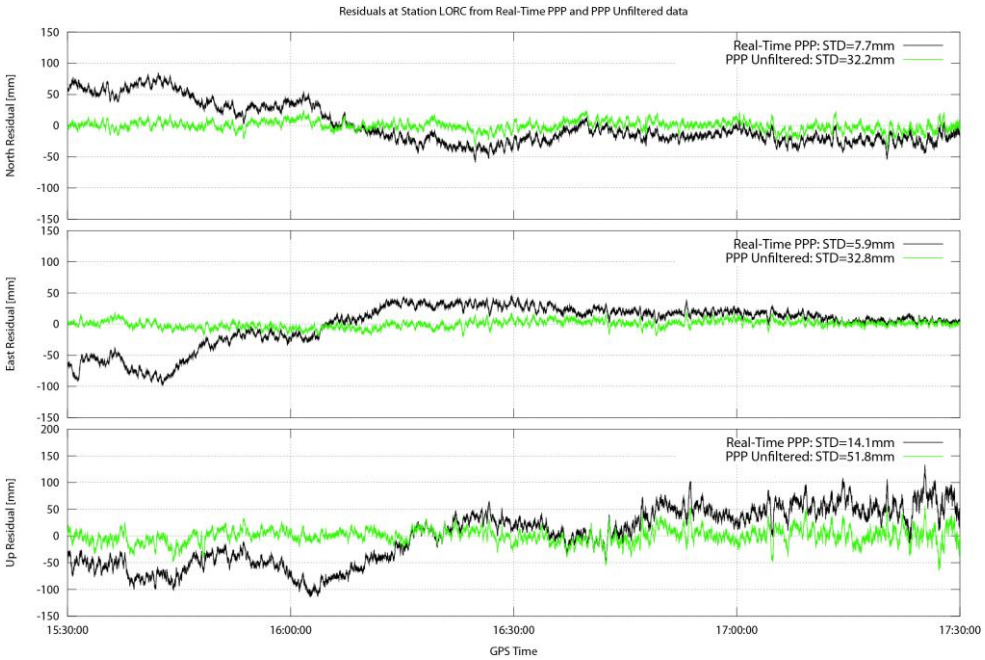


Fig. 9. Comparison of real-time and post-processed results for station LORC.

Within the first minutes of the considered timespan, the real-time solution clearly shows drifts in all coordinate components if compared to the reference solution (Fig. 9). Later, the solutions converge and show a very similar behaviour. The standard deviations computed over the timespan of 2 hours are 3 cm for the horizontal components and 5 cm in height. Thus, with the use of the real-time orbit and clock products, the solution precision decreased compared to the precision obtainable in post processing. The reason for the differences in the beginning of the presented period is that RTKPOST was not able to compute PPP solutions for some periods before 15:00 GPST because of bad data quality. As a consequence, the PPP method must reconverge first before having again its full precision. This is clearly a potential drawback of PPP. However, in general the running-in effect, generic for the PPP kinematic solutions based on Kalman filters, is no problem as long as a continuous processing is mantained.

Real-time and post-processed solutions show an identical behaviour during the earthquake (16:47-16:49 GPST). This means that the extraction of earthquake-related information would not have been adversely affected by the use of real-time products. Short-term transient effects and potential larger co-seismic offsets can be detected even if the absolute accuracy with respect to the global reference frame is not as good as with the final IGS products.

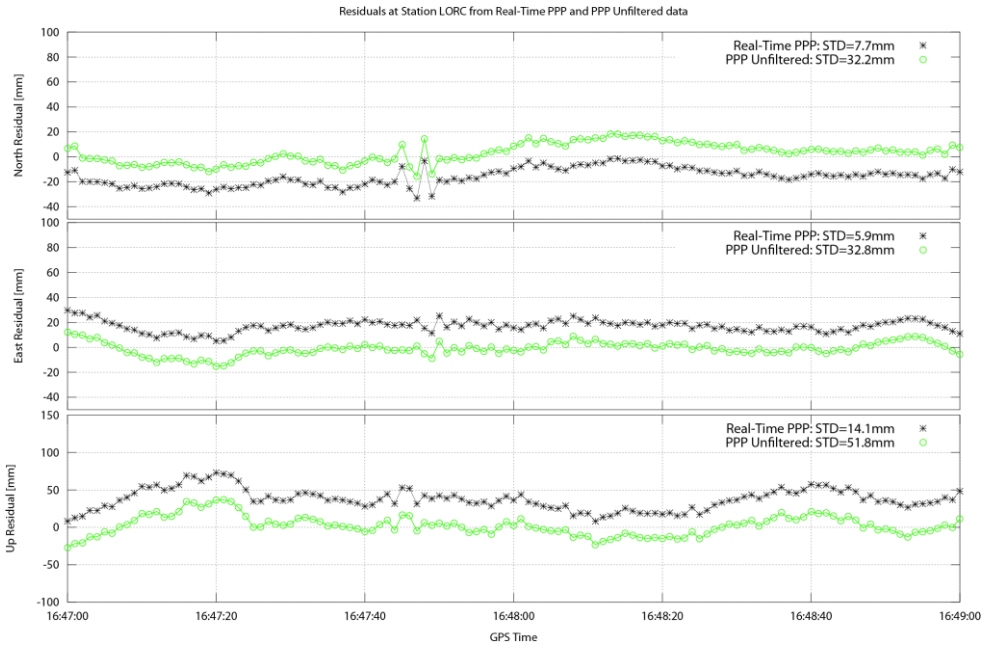


Fig. 10. Comparison of real-time and post-processing for the time of the earthquake (16:47:40 GPST) for station LORC.

## 6. Conclusions and Outlook

In this paper, we have compared two different GPS processing strategies in order to extract earthquake waves from the position time series of GPS stations. The approach of Relative Positioning (Bernese software) with subsequent Sidereal Filtering was compared to Precise Point Positioning (RTKLIB) in combination with Sidereal and Regional Filtering. These methods were used to analyze 1-Hz GPS observation data from Meristemum network recorded during the Lorca earthquake on May 11th, 2011 ($M_w = 5.1$). Both of them were shown to be able to deliver the short-term coordinate variations.

The filtering could considerably reduce the noise of the position time series. This leads to a better recognizability of the movements of the station caused by the seismic waves. The effectivity of Sidereal Filtering concerning the reduction of multipath effects could be validated. An additional Regional Filtering applied to the PPP solutions eventually led to better results (in terms of standard deviation, cf. Table 2) than the DD approach with Sidereal Filtering. This RF procedure was adapted to a high-rate GPS analysis using 1-Hz data.

We reached the goal of enhancing the visibility of seismic waves: Dynamic peak-to-peak displacements up to 3 cm, relatable to the seismic event, are clearly visible in the position time series of the station LORC (Fig. 7). The station direction of motion could be related to the direction of propagation of the seismic waves (Fig. 8). These results are consistent with the direction of rupture as described in Vissers and Meijninger (2011). The biggest foreshock and the time series of the other stations in the Meristemum network were considered as well, but no movement above noise level was visible after filtering.

A simulation of a real-time PPP processing shows that the quality of the data (observations, orbit and clock information) available in real time via NTRIP streams is comparable to the quality of the results from post processing. For the timespan of the earthquake, the solutions obtained by post processing and by real-time simulation are of the same quality (Fig. 10). Nonetheless, a general decrease in precision during the whole two hours considered is apparent. This is due to the used orbit and clock products. It is also to be noted that for a real-time application, the MSF and RF must be slightly modified, in order to be based only on the data prior to the event.

The PPP approach can deliver accurate absolute positions. Thus, even if all stations are affected by seismic displacements - implying that RF is no longer possible (cf. section 5.2) - the PPP approach without RF (in contrast to DD) is still able to deliver valid absolute positions for the monitoring process. This, as well as the suitability for real-time applications, can be regarded as an important advantage of this strategy.

The integration of PPP-based GPS positioning within a multisensor network can support the set-up of a reliable early warning system in the province of Murcia or any other region of interest. Integrating collocated GPS receivers and accelerometers could mitigate the problem of PPP reconvergence resulting from low-quality data or data gaps (cf. section 5.3) wich can be a problem of GPS-only

applications. Therefore, a further development of our methodology should be faced. Due to the real-time availability of GPS data via NTRIP streams, the scientific community can benefit from real-time position time series. For the operational use, the reliability and integrity of the streaming services has to be ensured. Such time series could be made available via a public access web-portal as described by Koppert (2011). GPS is the only sensor that allows a direct measurement of absolute station displacements. This information is the key contribution of GPS to earthquake analysis and can be obtained by a continuous monitoring of the positions of GPS stations.

Blewitt et al. (2009) show that an estimation of the direction of rupture as well as an approximation of the earthquake magnitude based on GPS timeseries is possible. In the future this could be based on the presented PPP approach instead of DD processing, getting a reliable tool for earthquake early-warning and monitoring systems.

**Acknowledgements**
This paper has been partially supported by the Spanish research projects TOPOIBERIA (CSD2006-00046) and ALERT-ES (CGL2010-19803-C03-02). We would also like to thank the Consejería de Agricultura y Agua of the Murcia Region (www.carm.es/cagric) and the International GNSS Service (Dow, et al. 2009) for the data they kindly provided via their public ftp service, and that has made this research possible.

**Abbreviations**
ANTEX - Antenna Exchange Format
ART: Aspect Repeat Time
ASPREP: Program to calculate the ART
CODE: Center for Orbit Determination in Europe
CRTG: GPS Station at Cartagena
CRVC: GPS Station at Caravaca de la Cruz
DD: Double Differencing
DOY: Day of Year
IGS: International GNSS Service
IGS-RTPP - IGS Real-Time Pilot Project
JUMI: GPS Station at Jumilla
LORC: GPS Station at Lorca
Meristemum: GPS Network from the Consejería de Agricultura y Agua of the Murcia Region
MSF: Modified Sidereal Filter
MURC: GPS Station at Murcia
NTRIP: Networked Transport of RTCM Data via Internet Protocol
PPP: Precise Point Positioning
RINEX: Receiver-INdependent Exchange
RF: Regional Filter

RTCM - Radio Technical Commission for Maritime Services
RTKLIB: Real-Time Kinematic LIBrary
RTKNAVI: Real-Time positioning utility of RTKLIB
RTKPOST: Post-Processing utility of RTKLIB
SALI: GPS Station at San Pedro del Pinatar
SP3(-c): Extended Standard Product 3 Orbit Format

**Bibliography**

AGNEW, D. C. & LARSON, K. (2007). Finding the repeat times of the GPS constellation. *GPS Solutions* 11, 71–76.

ALLEN, R. M. & ZIV, A. (2011). Application of real-time GPS to earthquake early warning. *Geophysical Research Letters* 38, L16310.

BEUTLER, G., BOCK, H., DACH, R., FRIDEZ, P., GÄDE, A., HUGENTOBLER, U., JÄGGI, A., MEINDL, M., MERVART, L., PRANGE, L., SCHAER, S., SPRINGER, T., URSCHL, C. & WALSER, P. (2008). *Bernese GPS Software ver. 5.0 Manual* [Online]. Astronomical Institute, University of Bern.

BLEWITT, G., HAMMOND, W. C., KREEMER, C., PLAG, H.-P., STEIN, S. & OKAL, E. (2009). GPS for real-time earthquake source determination and tsunami warning systems. *Journal of Geodesy* 83, 335-343.

BLEWITT, G., KREEMER, C., HAMMOND, W. C., PLAG, H.-P., STEIN, S. & OKAL, E. (2006). Rapid determination of earthquake magnitude using GPS for tsunami warning systems. *Geophysical Research Letters* 33, L11309.

BLEWITT, G., HAMMOND, W. C., KREEMER, C., PLAG, H.-P., STEIN, S. & OKAL, E. (2009). GPS for real-time earthquake source determination and tsunami warning systems. *Journal of Geodesys* 83, 335-343.

BOCK, Y., PRAWIRODIRDJO L. & MELBOURNE, T. I. (2004). Detection of arbitrarily large dynamic ground motions with a dense high-rate GPS network. *Geophysical Research Letters* 31, L06604.

BUFORN, E., SANZ DE GALDEANO, C. & UDÍAS, A. (1995). Seismotectonics of the Ibero-Maghrebian region. *Tectonophysics* 248, 247–261.

CABAÑAS -RODRÍGUEZ, L., CARREÑO-HERRERO, E., IZQUIERDO-ÁLVAREZ, A., MARTÍNEZ- SOLARES, J. M., DEL VILLAR, R. C., MARTÍNEZ-DÍAZ, J., BENITO-OTERINO, B., GASPAR-ESCRIBANO, J., RIVAS-MEDINA, A., GARCÍA-MAYORDOMO, J., PÉREZ-LÓPEZ, R., RODRÍGUEZ-PASCUA, M. A. & MURPHY-CORELLA, P. (2011). Informe del sismo de Lorca del 11 de mayo de 2011. *Technical report.* Instituto Geográfico Nacional de España.

CHOI, K., BILICH, A. L., LARSON, K. M. & AXELRAD, P. (2004). Modified sidereal filtering: Implications for high-rate GPS positioning. *Geophysical Research Letters* 31, L22608.

DETTMERING, D. & WEBBER, G. (2004). The EUREF-IP Ntrip Broadcaster: Real-time GNSS data for Europe. *Proceedings of the IGS2004 Workshop*. Astronomical Insitute, University of Bern, Switzerland. March 1-5, 2004.

DEMETS, C., GORDON, R. G., ARGUS, D. F. & STEIN, S. (1994). Effect of recent revisions to the geomagnetic reversal time scale on estimates of current plate motions. *Geophysical Research Letters* 21, 2191–2194.

DEWEY, J., PITMAN, W.C., RYAN, W.B.F. & BONNIN, J. (1973). Plate tectonics and the evolution of the Alpine system. *Bulletin of the Seismological Society of America* 84, 3137–3180.

DOW, J.M., NEILAN, R. E., & RIZOS, C., The International GNSS Service in a changing landscape of Global Navigation Satellite Systems. *Journal of Geodesy* (2009) 83:191–198.

FALCK, C., RAMATSCHI, M., SUBARYA, C., BARTSCH, M., MERX, A., HOEBERECHTS, J. & SCHMIDT, G. (2010). Near real-time GPS applications for tsunami early warning systems. *Natural Hazards and Earth System Science* 10, 181–189.

GARCÍA-MAYORDOMO, J., GASPAR-ESCRIBANO, J. M. & BENITO, B. (2007). Seismic hazard assessment of the Province of Murcia (SE Spain): analysis of source contribution to hazard. *Journal of Seismology* 11, 453–471.

GRAPENTHIN, R. & FREYMUELLER, J. T. (2011). The dynamics of a seismic wavefield: Animation and analysis of kinematic GPS data recorded during the 2011Tohoku-oki earthquake, Japan. *Geophysical Research Letters* 38, L18308.

KATO, T., TERADA, Y., ITO, K., HATTORI, R., ABE, T., MIYAKE, T., KOSHIMURA, S. & NAGAI, T. (2005). Tsunami due to the 2004 September 5th off the Kii Peninsula earthquake, Japan, recorded by new GPS buoy. *Earth Planets Space* 57, 297–301.

KHAZARADZE, G., SURIÑACH, E., GÁRATE, J. & DÁVILA, J. M. (2007). Crustal deformation in Eastern Betics from CuaTeNeo GPS network. *Geop. Res. Abstr*. 9.

KOPPERT, A. (2011). GPS-Seismometer auf Basis von NTRIP-Datenströmen. *Bachelor thesis* (in German). Institute of Geodesy, TU Darmstadt.

KOUBA, J. (2003). Measuring Seismic Waves Induced by Large Earthquakes with GPS. *Studia Geophysica et Geodaetica* 47, 741–755.

OHTA, Y., MEIANO, I., SAGIYA, T., KIMATA, F. & HIRAHARA, K. (2006). Large surface wave of the 2004 Sumatra-Andaman earthquake captured by the very long baseline kinematic analysis of 1-Hz GPS data. *Earth Planets Space* 58, 153–157.

PAPADOPOULOS, G. A. & FOKAEFS, A. (2005). Strong Tsunamis in the Mediterranean Sea: a re-evaluation. *Journal of Earthquake Technology* 42, 159–170.

POLLITZ, F. F., BÜRGMANN, R. & BANERJEE, P. (2011). Geodetic slip model of the 2011 Mw 9.0 Tohoku earthquake. *Geophysical Research Letters* 38, L00G08.

SCHMITZ, M. (2010). State Space Technology - Principle, RTCM Standardization and Examples. GNSS-reference networks. *QUO VADIS, 7th ALLSAT Open*, Hannover.

SØRENSEN, M. B., SPADA, M., BABEYKO, A., WIEMER, S. & GRÜNTHAL, G. (2012). Probabilistic tsunami hazard in the Mediterranean Sea. *Journal of Geophysical Research* 117, B01305.

TAKASU, T. (2011). RTKLIB ver. 2.4.1 Manual [Online]. Last checked 9.19.2011.

TINTI, S., ARMIGLIATO, A., PAGNONI, G. & ZANIBONI, F. (2005). Scenarios of Giant Tsunamis of Tectonic Origin in the Mediterranean. *Journal of Earthquake Technology* 42, 171-188.

VISSERS, R. L. M. & MEIJNINGER, B. M. L. (2011). The 11 May 2011 earthquake at Lorca (SE Spain) viewed in a structural-tectonic context. *Solid Earth* 2, 199–204.

WDOWINSKI, S., BOCK, Y., ZHANG, J., FANG, P. & GENRICH, J. (1997). Southern California Permanent GPS Geodetic Array: Spatial filtering of daily positions for estimating coseismic and postseismic displacements induced by the 1992 Landers earthquake. *Journal of Geophysical Research* 102, 18057–18070.

WEBER, G., GEBHARD, H. & KALAFUS, R. (2005). Networked Transport of RTCM via Internet Protocol (Ntrip). *IP-Streaming for Real-Time GNSS Applications*. Long Beach, CA.

YAMAZAKI, Y., LAY, T., CHEUNG, K. F., YUE, H. & KANAMORI, H. (2011). Modeling near-field tsunami observations to improve finite-fault slip models for the 11 March 2011 Tohoku earthquake. *Geophysical Journal International* 38, L00G15.

ZUMBERGE, J. F., HEFLIN, M. B., JEFFERSON, D. C., WATKINS, M. M. & WEBB, F. H. (1997). Precise Point positioning for the efficient and robust analysis of GPS data from large networks. *Journal of Geophysical Research* 102, 5005–5017.